Moment Forms Invariant to Rotation and Blur in Arbitrary Number of Dimensions

Jan Flusser, *Member*, *IEEE*, Jiří Boldyš, and Barbara Zitová, *Member*, *IEEE*

Abstract—We present the construction of combined blur and rotation moment invariants in arbitrary number of dimensions. Moment invariants to convolution with an arbitrary centrosymmetric filter are derived first, and then their rotationally invariant forms are found by means of group representation theory to achieve the desired combined invariance. Several examples of the invariants are calculated explicitly to illustrate the proposed procedure. Their invariance, robustness, and capability of using in template matching and in image registration are demonstrated on 3D MRI data and 2D indoor images.

Index Terms—N-D imaging, rotation invariants, blur invariants, group representation theory, image matching.

1 Introduction

1.1 Problem Formulation

Recognition of objects and patterns, regardless of their particular position, orientation, viewing angle, and of the degradations introduced by the imaging system is a very important task in computer vision, medical imaging, remote sensing, and in many other application areas. Finding a set of invariant descriptors is a key step to resolve this problem.

In many applications, there is a demand to recognize 3D objects directly rather than from their 2D projections. Since modern technologies like computer tomography, magnetic resonance imaging (MRI), and active range finders provide 3D (or even N-D) data, the derivation of the invariants in higher dimensions than two has become very important.

Invariants to imaging geometry have attracted the researchers' attention for many years. On the other hand, much less attention has been paid to invariants with respect to changes of the image intensity function (we call them radiometric invariants) and to combined radiometric-geometric invariants. An important class of radiometric degradations we are faced with, often in practice, is image blurring. Blurring can be caused by such factors like wrong focus of the camera, atmospheric turbulence, vibrations, and by sensor and/or scene motion to name a few. If the scene is flat, blurring can usually be described by a convolution $g = f * h$, where f is an original (ideal) image, g is an acquired image, and h is a point spread function (PSF) of the imaging system. Since in most practical tasks the PSF is unknown, having the invariants to convolution is of prime importance when recognizing objects in a blurred scene.

The aim of this paper is to propose a new class of invariants that are invariant to N-D object translation, rotation, and simultaneously, to convolution of the image function with an unknown centrosymmetric PSF (which can, for instance, describe the image blurring). This problem cannot be resolved just by a straightforward generalization or combination of previously published results because the rigid-body transform in N-D is much more complex in nature than that in 2D and, on the other hand, 3D geometric invariants published earlier cannot be easily extended to ensure convolution invariance.

1.2 Literature Survey

Numerous papers have been devoted to the invariants to rigid-body and affine transforms of spatial coordinates in 2D (see [1], [2] for a survey and other references). Among them, the methods based on image moments [3], [4], [5], [6], [7], [8], [9] play a significant role. In comparison with a large number of papers on 2D invariants, only few papers on 3D and/or N-D invariants have been published. The first attempt to extend 2D moment invariants to 3D was done by Sadjadi and Hall [10]. Probably, the first systematic approach to derivation of 3D moment invariants to rotation was published by Lo and Don [11]. It was based on group representation theory. Their results were later rediscovered (with some modifications) by Guo [12] and Galvez and Canton [13]. Guo's paper derived only three invariants without any possibility of their further extension. There have been several papers trying to generalize 3D rotational moment invariants either in the sense of the transformation group and/or in the sense of dimension. Reiss [14] used tensor algebra to derive 3D moment invariants to affine transform. He showed the invariants published in [10], [11] are just special cases of his descriptors. Another approach to deriving 3D affine invariants can be found in [15].

Markandey and deFigueiredo [16] tried to extend moment invariants to dimensions greater than three. They used the fundamental theorem from the classical paper [3]. As it was pointed out by Mamistvalov [17] and later by Reiss [18], this theorem contained some errors. However, these errors were incorporated also into [16]. Finally, Mamistvalov [19] published the correct version of the fundamental theorem of moment invariants in arbitrary dimensions and showed how to use it to derive N-D affine moment invariants (it should be

- *The authors are with the Institute of Information Theory and Automation, Academy of Sciences of the Czech Republic, 18208 Prague 8, Czech Republic. E-mail: {flusser, boldys, zitova}@utia.cas.cz.*
- *J. Boldyš is currently on leave at the Laboratory of Media Technology, Helsinki University of Technology, PL 6400, 02015 TKK, Finland.*

Manuscript received 19 Sept. 2001; revised 31 May 2002; accepted 1 Aug. 2002.
Recommended for acceptance by A. Khotanzad.
For information on obtaining reprints of this article, please send e-mail to: tpami@computer.org, and reference IEEECS Log Number 115012.

pointed out that a shorter version of this paper was published by the same author in a local journal 24 years earlier [20]).

Only few papers have been devoted to invariants with respect to changes of the image intensity function and to combined radiometric-geometric invariants. Most of them act in 2D only. Van Gool et al. introduced so-called affine-photometric invariants of gray level [21] and color [22] images. These features are invariant to the affine transform and to the linear change of contrast and brightness of the image simultaneously. Invariants to a rigid-body transform and contrast stretching based on normalized complex moments were proposed in [23]. Another set of combined rotation-photometric invariants that employ Zernike moments was described in [24].

A pioneer work on blur invariants was done by Flusser and Suk [25] who derived moment-based invariants to convolution with an arbitrary centrosymmetric PSF. From the geometric point of view, their descriptors were invariant to translation only. Despite this, these descriptors have found successful applications in face recognition on defocused photographs [26], in normalizing blurred images into the canonical forms [27], [28], in template-to-scene matching of satellite images [25], in blurred digit recognition [29], and in focus/defocus quantitative measurement [30]. A significant improvement motivated by a problem of registration of blurred images was made by Flusser and Zitová. They introduced 2D combined blur-rotation invariants [31] and reported their successful usage in satellite image registration [32]. However, all of the blur and combined invariants mentioned above are defined in 2D only. The first set of N-D blur invariants was introduced by Flusser et al. [33], but these features were just shift invariant. Thus, their practical utilization was substantially limited. Because of more complicated nature of rotation in higher dimensions, the method used for derivation of 2D invariants [31] cannot be generalized.

1.3 Paper Organization

In this paper, we propose a new class of combined blur-rotation moment invariants defined in arbitrary dimensions. The derivation of these invariants is based on group representation theory. In Section 2, basic definitions are given. Invariants to convolution of an N-D image with a centrosymmetric PSF are introduced in Section 3. In Section 4, we briefly recall the basic terms of the group representation theory. This theory is employed in Section 5 to derive the combined invariants to rotation and convolution. Section 6 demonstrates numerical properties of the invariants and their practical utilization in 3D and 2D cases.

2 Basic Definitions and Notation

In this section, we introduce some basic definitions which will be used later in the paper.

Notation. For $N \geq 1$, given the $x_i \in \mathcal{R}$, $p_i \in \mathcal{N}_0$, $k_i \in \mathcal{N}_0$ ($\mathcal{R}$ and $\mathcal{N}_0$ denote the sets of real numbers and nonnegative integers, respectively). Then,

$$\mathbf{x} \equiv (x_1, \cdots, x_N)^T$$

denotes N-dimensional vector of coordinates and

$$\mathbf{p} \equiv (p_1, \cdots, p_N)^T, \qquad \mathbf{k} \equiv (k_1, \cdots, k_N)^T$$

denote N-dimensional vectors of parameters. Logical relations are defined analogically to

$$\mathbf{p} < \mathbf{k} \iff p_i < k_i \quad i = 1, \cdots, N.$$

The following notation is further introduced:

$$\mathbf{dx} \equiv dx_1 \cdots dx_N,$$
$$|\mathbf{p}| \equiv \sum_{i=1}^{N} p_i,$$
$$\mathbf{x}^{\mathbf{p}} \equiv \prod_{i=1}^{N} x_i^{p_i},$$
$$\mathbf{p}! \equiv \prod_{i=1}^{N} (p_i!),$$
$$\binom{\mathbf{p}}{\mathbf{k}} \equiv \prod_{i=1}^{N} \binom{p_i}{k_i}.$$

Definition 1. *By N-dimensional image function (or image), we understand any real function $f(\mathbf{x})$ having a bounded support and finite nonzero integral.*

Definition 2. *Ordinary geometric moment $m_{\mathbf{p}}^{(f)}$ of order $|\mathbf{p}|$ of the image $f(\mathbf{x})$ is defined by the integral*

$$m_{\mathbf{p}}^{(f)} = \int_{R^N} \mathbf{x}^{\mathbf{p}} f(\mathbf{x}) \mathbf{dx}. \tag{1}$$

Definition 3. *Fourier transform (or spectrum) $F(\mathbf{u})$ of the image $f(\mathbf{x})$ is defined as*

$$F(\mathbf{u}) = \int_{R^N} f(\mathbf{x}) e^{-2\pi i \mathbf{u}^{\mathbf{T}} \mathbf{x}} \mathbf{dx}, \tag{2}$$

where i is the imaginary unit.

Note that the Fourier transform as well as the moments of all orders exist for any image function.

Lemma 1. *The relationship between Fourier transform and geometric moments of an image is expressed by the following equation:*

$$F(\mathbf{u}) = \sum_{\mathbf{0} \leq \mathbf{k}} \frac{(-2\pi i)^{|\mathbf{k}|}}{\mathbf{k}!} m_{\mathbf{k}}^{(f)} \mathbf{u}^{\mathbf{k}}. \tag{3}$$

The assertions of Lemma 1 can be easily proven just using the definitions of moments and of the Fourier transform.

3 Blur Invariants

In this section, a set of moment forms invariant to image blurring is derived. In the following text, the blur invariance is understood as invariance to convolution with centrally symmetric PSF:

$$h(\mathbf{x}) = h(-\mathbf{x}). \tag{4}$$

This is a natural choice because most real degradations such as out-of-focus blur, atmospheric turbulence blur, etc., fulfill the constraint of centrosymmetry.

The following two theorems are of fundamental importance.

Theorem 1. *Tangent of the Fourier transform phase is a blur invariant.*

To prove this theorem, it is sufficient to realize that the phase of the Fourier transform of $h(\mathbf{x})$, as of centrally symmetrical function, can equal only 0 or π.

Theorem 2. *Tangent of the Fourier transform phase of any image $f(\mathbf{x})$ can be expanded into power series (except of the points in which $F(\mathbf{u}) = 0$ or $\mathrm{ph}\ F(\mathbf{u}) = \pm\pi/2$)*

$$\tan(\mathrm{ph}\ F(\mathbf{u})) = \frac{\mathrm{Im}\ F(\mathbf{u})}{\mathrm{Re}\, F(\mathbf{u})} = \sum_{\mathbf{0}\le\mathbf{k}} c_{\mathbf{k}}\mathbf{u}^{\mathbf{k}}, \tag{5}$$

where the $c_{\mathbf{k}}$'s are also blur invariants.

Proof. The $\tan(\mathrm{ph}\ F(\mathbf{u}))$ is the ratio of two absolutely convergent power series, thus it can be also expressed as a power series. The invariance of $c_{\mathbf{k}}$'s follows from comparison of the coefficients of the same monomials $\mathbf{u}^{\mathbf{k}}$.□

The coefficients $c_{\mathbf{k}}$ can be straightforwardly derived. It follows from the substitution of (3) into (5) that

$$\sum_{\substack{\mathbf{0}\le\mathbf{k}\\ |\mathbf{k}|\mathrm{odd}}} \frac{(-1)^{(|\mathbf{k}|-1)/2}(-2\pi)^{|\mathbf{k}|}}{\mathbf{k}!} m_{\mathbf{k}}\mathbf{u}^{\mathbf{k}} = \sum_{\substack{\mathbf{0}\le\mathbf{j}\\ |\mathbf{j}|\mathrm{even}}} \frac{(-1)^{|\mathbf{j}|/2}(-2\pi)^{|\mathbf{j}|}}{\mathbf{j}!} m_{\mathbf{j}}\mathbf{u}^{\mathbf{j}} \sum_{\mathbf{0}\le\mathbf{n}} c_{\mathbf{n}}\mathbf{u}^{\mathbf{n}}.$$

Comparison of the coefficients of the same monomials $\mathbf{u}^{\mathbf{p}}$ reveals that $c_{\mathbf{k}} = 0$ for $|\mathbf{k}|$ even. The same comparison for one particular odd-order $|\mathbf{p}|$ of the monomial $\mathbf{u}^{\mathbf{p}}$ gives

$$\frac{(-1)^{(|\mathbf{p}|-1)/2}(-2\pi)^{|\mathbf{p}|}}{\mathbf{p}!} m_{\mathbf{p}} = m_{\mathbf{0}}c_{\mathbf{p}} + \sum_{\substack{\mathbf{0}\le\mathbf{n}\le\mathbf{p}\\ 0<|\mathbf{n}|<|\mathbf{p}|}} \frac{(-1)^{|\mathbf{n}|/2}(-2\pi)^{|\mathbf{n}|}}{\mathbf{n}!} m_{\mathbf{n}}c_{\mathbf{p}-\mathbf{n}}.$$

Definition 1 guarantees that $m_{\mathbf{0}} \neq 0$. Therefore, it is possible to express $c_{\mathbf{p}}$ as

$$c_{\mathbf{p}} = \frac{(-1)^{(|\mathbf{p}|-1)/2}(-2\pi)^{|\mathbf{p}|}}{\mathbf{p}!}\frac{m_{\mathbf{p}}}{m_{\mathbf{0}}} - \frac{1}{m_{\mathbf{0}}} \sum_{\substack{\mathbf{0}\le\mathbf{n}\le\mathbf{p}\\ 0<|\mathbf{n}|<|\mathbf{p}|}} \frac{(-1)^{|\mathbf{n}|/2}(-2\pi)^{|\mathbf{n}|}}{\mathbf{n}!} m_{\mathbf{n}}c_{\mathbf{p}-\mathbf{n}}.$$

Using a simplified notation

$$Q_{\mathbf{p}} \equiv \frac{c_{\mathbf{p}}\mathbf{p}!}{(-1)^{(|\mathbf{p}|-1)/2}(-2\pi)^{|\mathbf{p}|}}, \tag{6}$$

we get the recursive formula

$$\begin{aligned} Q_{\mathbf{p}} &= \frac{m_{\mathbf{p}}}{m_{\mathbf{0}}} - \frac{1}{m_{\mathbf{0}}} \sum_{\substack{\mathbf{0}\le\mathbf{n}\le\mathbf{p}\\ 0<|\mathbf{n}|<|\mathbf{p}|}} \binom{\mathbf{p}}{\mathbf{n}} Q_{\mathbf{p}-\mathbf{n}}m_{\mathbf{n}} \qquad \text{for odd } |\mathbf{p}|,\\ Q_{\mathbf{p}} &= 0 \qquad \text{for even } |\mathbf{p}|. \end{aligned} \tag{7}$$

Equation (7) enables to calculate moment forms $Q_{\mathbf{p}}$ (and also $c_{\mathbf{p}}$ with further use of (6)) which are invariant under convolution with a centrally symmetrical kernel.

4 Recalling the Basic Terms of the Group Representation Theory

The goal of this section is to recall basic terms of the group representation theory, which are further used when deriving rotation invariants. A few explanations and remarks are added to simplify understanding for the readers who are not familiar with this theory. Due to the space limitations and to keep the text readable, we stay at the intuitive level only. However, in case of deeper interest in this field, the readers are encouraged to consult some standard textbook, e.g., [34].

An essential operation for further consideration is the rotation of the image. Let $R(a)$ be 2D rotation around the origin where a is the angle of rotation, $0 \le a < 2\pi$. Composition of two consequent rotations is also a rotation

$$R(a) \circ R(b) = R(a+b),$$

where angle addition is considered modulo 2π. Clearly, rotation by zero degrees plays the role of unit element, while rotation by $(2\pi - a)$ is an inverse of $R(a)$.

Analogous characteristics are typical, not only for the rotations but also for other geometric or algebraic objects. Such objects can be called elements of a certain group.

Definition 4. *Any set ξ with an operation $\circ$ (called multiplication) is called group if and only if*

1. *ξ is closed with respect to multiplication $\circ$, i.e.,*
$$G_a, G_b \in \xi \quad \Rightarrow \quad G_a \circ G_b \in \xi,$$
2. *The multiplication is associative, i.e., for any a, b, c*
$$(G_a \circ G_b) \circ C_c = G_a \circ (G_b \circ C_c),$$
3. *There exists a unit $E \in \xi$ such that for any a*
$$E \circ G_a = G_a, \quad G_a \circ E = G_a,$$
4. *For every $G_a \in \xi$, there exists an inverse element $G_a^{-1} \in \xi$ such that*
$$G_a \circ G_a^{-1} = E, \quad G_a^{-1} \circ G_a = E.$$

Now, we can refer to the two-dimensional rotations as to a continuous (because of the parameter a) group, which we denote SO(2). SO(2) is so-called Abelian group because its elements commute. An example of a group whose elements do not commute is the group SO(3) of all rotations in 3D space around any given point. Its elements are rotations $R_{\mathbf{k}}(a)$ of an angle a around a vector $\mathbf{k}$ arising from the central point.

In practice, the rotations act on some objects which are elements of a vector space L (L may be "traditional" Euclidean space R^2 for instance). Any rotation can be then represented by a linear operator on L. Now, we can naturally define the representation of a group.

Definition 5. *A set of linear operators $T(G_a)$, $G_a \in \xi$ on a vector space L is called representation of the group ξ in the space L, if it corresponds to the group elements such that*

$$T(G_a) \circ T(G_b) = T(G_a \circ G_b), \qquad T(E) = 1.$$

Once we choose a basis $\mathbf{e}_1, \mathbf{e}_2, \ldots, \mathbf{e}_s$ in the space L, every linear operator $T(G_a)$ can in this basis be represented by a matrix $T_{ji}(G_a)$, satisfying

$$T(G_a)\mathbf{e}_i = \sum_j T_{ji}(G_a)\mathbf{e}_j. \tag{8}$$

Thus, we get matrix representation of the group.

The usual way of simplifying many kinds of algebraic problems is to find a basis in which the corresponding matrix will have some simplified form. In this paper, we want to make the matrix block-diagonal:

$$\begin{pmatrix} T^{(1)} & 0 & 0 & \ldots \\ 0 & T^{(2)} & 0 & \ldots \\ 0 & 0 & T^{(3)} & \ldots \\ \vdots & \vdots & \vdots & \ddots \end{pmatrix}. \tag{9}$$

The $T^{(i)}$s are the blocks of the matrix representation T and they are therefore representations themselves. They operate on invariant subspaces L_i of the space L

$$L = L_1 + L_2 + L_3 + \ldots \quad .$$

After application of $T^{(i)}$ on an element from L_i, we get a linear combination of elements from L_i again.

Thus, the representation $T(G_a)$, $G_a \in \xi$, is said to be reducible and can be decomposed into its irreducible components

$$T(G_a) = T^{(1)}(G_a) \oplus T^{(2)}(G_a) \oplus T^{(3)}(G_a) \oplus \ldots. \tag{10}$$

Definition 6. *Given the space L invariant under operators $T(G_a)$ of the representation of group ξ. If any mutually orthogonal subspaces L_1 and L_2 of L are both invariant under $T(G_a)$ for all $G_a \in \xi$, then the representation $T(G_a)$, $G_a \in \xi$, is called reducible, otherwise it is called irreducible.*

If one of the blocks in (9) has size 1×1 and equals 1, then the corresponding basis function is invariant to the operator T. The main idea of the presented method has thus been exposed: to find a function invariant to rotation, a function which under the rotation operator is transformed according to a 1×1 matrix of a single 1.

As an example, we present irreducible representations of the group SO(2) (every particular m generates a different representation):

$$T^{(m)}(a) = \exp(-ima), \qquad m = 0, \pm 1, \pm 2, \ldots \quad . \tag{11}$$

Because SO(2) is an Abelian group, the irreducible representations are one-dimensional.

Given the space of functions $\psi(r, \varphi)$ defined on the R^2 plane and expressed in polar coordinates r, φ in 2D. In this space, the irreducible representations (11) of the group SO(2) have basis functions

$$\psi^m = \exp(im\varphi), \qquad m = 0, \pm 1, \pm 2, \ldots \quad . \tag{12}$$

At this point, one remark is worth mentioning: We get the basis functions with positive (resp. with negative) m, if we express the functions $\psi^m = (x + iy)^m$ (respectively, the functions $\psi^m = (x - iy)^m$) in polar coordinates. Popular complex moments [4] are projections of the image function on these basis functions of one-dimensional irreducible representations of SO(2) group. This is the reason why the complex moments can be used for deriving 2D rotation invariants in a straightforward way [35].

Irreducible representations of the group SO(3) are more complicated. They are usually denoted as $D^{(j)}$, $j = 0, 1, 2, \ldots$. The dimension of $D^{(j)}$ is $2j + 1$. Thus, for $j = 0, 1, 2, \ldots$ we get dimensions $1, 3, 5, \ldots$. The possible dimensions determine how a representation of the group SO(3) is decomposed, see (10).

The $D^{(j)}$'s could be also used as representations for the group SO(2) elements, but then they are already reducible:

$$D^{(\ell)} = \sum_{m=-\ell}^{m=\ell} T^{(m)}.$$

At this point, this fact may not be important itself, but it determines indexing of so-called spherical harmonics

$$Y_m^\ell(\vartheta, \varphi), \qquad m = -\ell, -\ell + 1, \ldots, \ell - 1, \ell. \tag{13}$$

Given the space of functions $\psi(r, \vartheta, \varphi)$ defined on R^3 space and expressed in spherical coordinates r, ϑ, φ. Then, the set of spherical harmonics (13) for one particular ℓ is basis of the irreducible representation $D^{(\ell)}$.

What to do, if our particular representation does not contain in its decomposition $T^{(0)}$ for SO(2), respectively, $D^{(0)}$ for SO(3)? Basis functions of other irreducible representations are not invariants. Fortunately, we can also investigate transformational properties of products of the currently used basis functions. Moreover, there is a deterministic way of multiplying them so that we can be sure we get the desired result.

Given a set of s_α basis functions $\varphi_k^{(\alpha)}$ of irreducible representation $T^{(\alpha)}$. That means that $\varphi_k^{(\alpha)}$'s are under the operation of $T^{(\alpha)}$ transformed in accordance with (8). Given then, a set of s_β basis functions $\psi_\ell^{(\beta)}$ of irreducible representation $T^{(\beta)}$. Then, according to (8), the set of $s_\alpha s_\beta$ functions $\{\varphi_k^{(\alpha)}\psi_\ell^{(\beta)}\}$ is transformed as

$$\begin{aligned} T\left\{\varphi_k^{(\alpha)}\psi_\ell^{(\beta)}\right\} &= \sum_i \sum_j T_{ik}^{(\alpha)} T_{j\ell}^{(\beta)} \left\{\varphi_i^{(\alpha)}\psi_j^{(\beta)}\right\} \\ &\equiv \sum_{ij} T_{ij,k\ell}^{(\alpha\times\beta)} \left\{\varphi_i^{(\alpha)}\psi_j^{(\beta)}\right\}. \end{aligned}$$

It can be verified that

$$T_{ij,k\ell}^{(\alpha\times\beta)} \equiv T_{ik}^{(\alpha)} T_{j\ell}^{(\beta)}$$

is also a matrix representation. The multiplication operation between the two representations is called tensor product and operator-like it is denoted as

$$T^{(\alpha)} \otimes T^{(\beta)} \equiv T^{(\alpha\times\beta)}.$$

Generally, the tensor product of two irreducible representations $T^{(\alpha)}$ and $T^{(\beta)}$ can be reducible:

$$T^{(\alpha\times\beta)} = \sum T^{(\gamma)}. \tag{14}$$

Then, it is desirable to find such linear combination of functions $\{\varphi_i^{(\alpha)}\psi_j^{(\beta)}\}$ (we denote them as $\Psi_k^{(\gamma)}$) which are transformed according to the irreducible representation $T^{(\gamma)}$:

$$\Psi_k^{(\gamma)} = \sum_{ij} C(\alpha\beta\gamma, ijk)\left\{\varphi_i^{(\alpha)}\psi_j^{(\beta)}\right\}. \quad (15)$$

The $C(\alpha\beta\gamma, ijk)$'s are called Clebsch-Gordan coefficients and they can be found in the group theory related literature. They are also implemented, together with spherical harmonics, in advanced symbolic manipulation software systems like MATHEMATICA.

In this paper, we need to know what is the decomposition of the tensor products of two irreducible representations of SO(2), respectively, SO(3). We can then use these relations to get among others, irreducible representation $T^{(0)}$, respectively, $D^{(0)}$, in the decomposition, and consequently, the invariant basis function. The following equality holds for SO(2):

$$T^{(m_1)} \otimes T^{(m_2)} = T^{(m_1+m_2)}. \quad (16)$$

Tensor product of two irreducible representations of SO(3) equals

$$D^{(j_1)} \otimes D^{(j_2)} = \sum_{J=|j_1-j_2|}^{J=j_1+j_2} D^{(J)}. \quad (17)$$

Thus, we can combine, e.g., $D^{(2)}$ and $D^{(2)}$ to get $D^{(0)}$

$$D^{(2)} \otimes D^{(2)} = D^{(0)} \oplus D^{(1)} \oplus D^{(2)} \oplus D^{(3)} \oplus D^{(4)}$$

and, by means of (15), find invariant

$$\Psi_0^{(0)} = \sum_{i,j=-2}^{2} C(220, ij0)\{\varphi_i^{(2)}\psi_j^{(2)}\}.$$

5 Combined Invariants to Rotation and Convolution

In Section 3, the way to calculate the pure invariants to image blurring in arbitrary dimensions was explained. In Section 4, the theoretical background to deriving rotation invariants was given. In this section, we employ the group representation theory to derive combined invariants to rotation and convolution. They represent qualitatively new classes of invariants that have not been reported yet.

Equation (5), which generates the blur invariants $c_{\mathbf{k}}$, is a natural starting point for investigation of the rotation invariance. The comparison of (3) and (5) reveals parallelism between the expansions into the power series of the Fourier transform and of the tangent of its phase. The first expansion generates image moments and the second expansion, which is itself blur invariant, generates moment blur invariants. Further investigation also shows analogous rotational properties of (3) and (5). The rotational properties of the Fourier transform were used in [11] to calculate forms of moments invariant under the rotation in 3D case. The mentioned analogy offers to use the same technique, generalized to N-D, to calculate forms of blur invariants which are then invariant also under the rotation.

The method mentioned above takes advantage of the transformational properties of $\tan(\mathrm{ph}F(\mathbf{u}))$. If we rotate in (2), both spatial and spectral coordinates by the same rotation operator R,

$$\mathbf{u}' = R\mathbf{u}, \qquad \mathbf{x}' = R\mathbf{x},$$

we get again the Fourier transform of the rotated image, expressed in the rotated spectral coordinates. It reflects the fact that, if the image is rotated, the same is true for its Fourier transform. Calculating the phase (and, consequently, the phase tangent) does not change this relation. Thus, from (5) we get

$$\sum_{\mathbf{0}\le\mathbf{k}} c_{\mathbf{k}}\mathbf{u}^{\mathbf{k}} = \sum_{\mathbf{0}\le\mathbf{k}} c'_{\mathbf{k}}\mathbf{u}'^{\mathbf{k}}, \quad (18)$$

where the $c'_{\mathbf{k}}$'s are functions of the rotated image $f(\mathbf{x}')$.

Equation (18) is a kind of invariance relation. The left-hand side reflects the state before rotation, the right-hand side after rotation. If the monomial $\mathbf{u}^{\mathbf{k}}$ of certain order $|\mathbf{k}|$ is rotated, we get a linear combination of monomials of the same order (we never get cubic monomial from a quadratic one, for instance). The monomials of the same order are transformed among themselves. Therefore, we can decompose (18) so that each order $|\mathbf{k}| = p$ corresponds to one individual equation:

$$\sum_{\substack{\mathbf{0}\le\mathbf{k}\\ |\mathbf{k}|=p}} c_{\mathbf{k}}\mathbf{u}^{\mathbf{k}} = \sum_{\substack{\mathbf{0}\le\mathbf{k}\\ |\mathbf{k}|=p}} c'_{\mathbf{k}}\mathbf{u}'^{\mathbf{k}}. \quad (19)$$

For example, (19) for $p = 2$ contains only quadratic monomials. From (19), it is now obvious that the blur invariants $c_{\mathbf{k}}$ of the same order are also transformed among themselves.

It is advantageous to introduce the following vector notation:

$$\sum_{\substack{\mathbf{0}\le\mathbf{n}\\ |\mathbf{n}|=p}} c_{\mathbf{n}}\mathbf{u}^{\mathbf{n}} \equiv \mathbf{C}_p^T\mathbf{U}_p, \quad (20)$$

where proper order of elements of the column vectors

$$\mathbf{C}_p = \{c_{\mathbf{n}}\}_{|\mathbf{n}|=\mathrm{p}}, \qquad \mathbf{U}_p = \{\mathbf{u}^{\mathbf{n}}\}_{|\mathbf{n}|=\mathrm{p}},$$

has to be maintained to fulfill (20). Equation (19) can be now rewritten to

$$\mathbf{C}_p^T\mathbf{U}_p = \mathbf{C}_p'^T\mathbf{U}'_p. \quad (21)$$

Elements of $\mathbf{U}_p$ form a basis of a space invariant under rotation. There is a matrix relation between the left-side $\mathbf{U}_p$ and the right-side $\mathbf{U}'_p$ for an arbitrary rotation. But this matrix is generally complicated. To simplify it, we must use the results of the preceding section. We must use a better basis of this space—a basis of irreducible representations of a group of rotations. We denote it $\mathbf{b}_p$. Relation between the old and new bases is described by means of transition matrix A_p:

$$\mathbf{U}_p = A_p\mathbf{b}_p. \quad (22)$$

If we introduce the following vectors $\mathbf{f}_p$ of forms of $c_{\mathbf{n}}$'s

$$\mathbf{f}_p = A_p^+\mathbf{C}_p, \quad (23)$$

then the shape of (20) is preserved

$$\mathbf{C}_p^T\mathbf{U}_p = \mathbf{f}_p^+\mathbf{b}_p$$

and we get a new relation

$$\mathbf{f}_p^+\mathbf{b}_p = \mathbf{f}_p'^+\mathbf{b}'_p.$$

The relation between $\mathbf{b}_p$ and $\mathbf{b}'_p$ is now described by block-diagonal matrix. Considering unitarity of the rotation

operator, the same is true for $\mathbf{f}_p$ and $\mathbf{f}'_p$. Each block corresponds to a particular irreducible representation of the rotation group. Moreover, we know which elements of $\mathbf{f}_p$ are transformed according to which particular irreducible representations. Therefore, in light of Section 4, we can find forms of $c_{\mathbf{k}}$'s invariant to rotation. Because $c_{\mathbf{k}}$'s are already invariant to blur, we automatically obtain the desired combined invariance.

For completeness, one more point should be mentioned. The decomposition of (18) into the sums of monomials of the same order is not necessary. It just significantly simplifies further analysis. However, we must be aware that if looking for invariants, it is possible to perform tensor product of irreducible representations operating on different spaces. It provides the possibility to construct invariants containing elements of forms $\mathbf{f}_p$ of different orders (consequently, moments of different orders).

In the two following sections, the examples of calculating invariants are presented both in 2D and 3D case (the invariants in dimensions greater than three can be calculated analogously). The order $p = 3$ was chosen because it is the first practically important order and its description is still simple enough ($c_{\mathbf{p}} = 0$ for $|\mathbf{p}| = 0$ and $|\mathbf{p}| = 2$, see (7); $c_{\mathbf{p}} = 0$ for $|\mathbf{p}| = 1$ because, in the following examples, we use central moments instead of ordinary moments to ensure shift invariance). The derivation of some invariants in 2D is presented just for illustration of the used method. Being a particular case, 2D combined invariants can be derived without knowledge of the group representation theory [31].

5.1 Examples of Calculating 2D Invariants

1. Specification of vectors $\mathbf{C}_p$ and $\mathbf{U}_p$ from (20).

$$\mathbf{U}_3 = (u_1^3, u_1^2 u_2, u_1 u_2^2, u_2^3)^T,$$
$$\mathbf{C}_3 = (c_{30}, c_{21}, c_{12}, c_{03})^T.$$

2. Specification of the basis $\mathbf{b}_p$ from (22). As it was already explained, the functions (12)

$$b^m = \exp(im\varphi), \qquad m = 0, \pm 1, \pm 2, \ldots$$

are bases of one-dimensional irreducible representations $T^{(m)}$ of group SO(2). After substitution of polar coordinates into $\mathbf{U}_3$, it is obvious that elements of new basis $\mathbf{b}_3$ are

$$\mathbf{b}_3 = (b^3, b^1, b^{-1}, b^{-3})^T,$$

i.e., they are the bases of irreducible representations $T^{(3)}$, $T^{(1)}$, $T^{(-1)}$, and $T^{(-3)}$. Relationship between Cartesian and polar coordinates is

$$u_1 = r\cos\varphi,$$
$$u_2 = r\sin\varphi.$$

We put $r = 1$ because rotational properties are not dependent on the value of radial component r and its presence in further calculations rather disturbs.

3. Calculation of the transition matrix A_p according to (22). As a result of the previous step we get the transition matrix

$$A_3 = \frac{1}{8}\begin{pmatrix} 1 & 3 & 3 & 1 \\ -i & -i & i & i \\ -1 & 1 & 1 & -1 \\ i & -3i & 3i & -i \end{pmatrix}.$$

4. Calculation of the forms $\mathbf{f}_p$ according to (23) by means of (6) and (7). The elements of a new vector of forms $\mathbf{f}_3$ are

$$f_3^3 = \frac{\pi^3\,(-i\,m_{03} - 3\,m_{12} + 3\,i\,m_{21} + m_{30})}{6\,m_{00}},$$
$$f_3^1 = \frac{\pi^3\,(i\,m_{03} + m_{12} + i\,m_{21} + m_{30})}{2\,m_{00}},$$
$$f_3^{-1} = \frac{\pi^3\,(-i\,m_{03} + m_{12} - i\,m_{21} + m_{30})}{2\,m_{00}},$$
$$f_3^{-3} = \frac{\pi^3\,(i\,m_{03} - 3\,m_{12} - 3\,i\,m_{21} + m_{30})}{6\,m_{00}}.$$

They are also transformed according to the irreducible representations $T^{(3)}$, $T^{(1)}$, $T^{(-1)}$, and $T^{(-3)}$.

5. Explanation and examples. The invariants are only such functions which are transformed according to the irreducible representation $T^{(0)}$. Otherwise, they are always multiplied by a factor depending on the angle of rotation, see (11). The representation $T^{(0)}$ we can get, for example, as a tensor product

$$T^{(3)} \otimes T^{(-3)} = T^{(0)},$$

see (16). The form transforming according to this tensor product is in one-dimensional case just simple product of the forms f_3^3 and f_3^{-3}, which are transforming according to the representations $T^{(3)}$ and $T^{(-3)}$.

As the examples of the results, a set of invariants containing moments of the third order is presented. The relevant tensor products of irreducible representations are denoted on the left side. Constants with respect to the rotation are omitted.

$$T^{(3\times-3)} : f_3^3 f_3^{-3} = ({m_{03}}^2 + 9\,{m_{12}}^2 - 6\,m_{03}\,m_{21} + 9\,{m_{21}}^2 - 6\,m_{12}\,m_{30} + {m_{30}}^2)/{m_{00}}^2$$
$$T^{(1\times-1)} : f_3^1 f_3^{-1} = ({m_{03}}^2 + {m_{12}}^2 + 2\,m_{03}\,m_{21} + {m_{21}}^2 + 2\,m_{12}\,m_{30} + {m_{30}}^2)/{m_{00}}^2$$
$$T^{(3\times-1\times-1\times-1)} : f_3^3 {f_3^{-1}}^3 = (m_{03} - 3\,i\,m_{12} - 3\,m_{21} + i\,m_{30})\,(m_{03} + i\,m_{12} + m_{21} + i\,m_{30})^3/{m_{00}}^4$$

The last invariant is complex. For practical calculations it is suitable to take apart real and imaginary parts.

Since the blur invariants of even orders do not exist and since the first-order invariants are meaningless, these invariants are the simplest combined invariants. It is worth noting that they correspond to the well-known pure rotation invariants [3]. This is because the third-order moments themselves are invariant to convolution. However, this is not true

for higher orders and the explicit formulae of combined invariants are much more complicated.

5.2 Examples of Calculating 3D Invariants

1. Specification of vectors $\mathbf{C}_p$ and $\mathbf{U}_p$ from (20).

$$\mathbf{U}_3 = (u_1^3, u_2^3, u_3^3, u_1^2u_2, u_1^2u_3, u_1u_2^2, u_2^2u_3, u_1u_3^2, u_2u_3^2, u_1u_2u_3)^T$$
$$\mathbf{C}_3 = (c_{300}, c_{030}, c_{003}, c_{210}, c_{201}, c_{120}, c_{021}, c_{102}, c_{012}, c_{111})^T$$

2. Specification of the basis $\mathbf{b}_p$ from (22). As it was mentioned above, the spherical harmonics (13) are for one particular nonnegative integer ℓ basis of irreducible representation $D^{(\ell)}$ of group SO(3). Thus, the new basis $\mathbf{b}_3$ will be formed by some of the elements:

$$b^{\ell,m} = Y_m^\ell(\vartheta,\varphi), \quad \ell = 0,1,2,\ldots,$$
$$m = -\ell, -\ell+1, \ldots, \ell-1, \ell.$$

The dimension of the representation $D^{(\ell)}$ is $2\ell+1$. In accordance with the dimension of $\mathbf{U}_3$, the new basis $\mathbf{b}_3$ must contain 10 elements. Therefore, it is easy to realize that $\mathbf{b}_3$ contains basis elements of irreducible representations $D^{(3)}$ and $D^{(1)}$:

$$\mathbf{b}_3 = (b^{3,3}, b^{3,2}, b^{3,1}, b^{3,0}, b^{3,-1}, b^{3,-2}, b^{3,-3}, b^{1,1}, b^{1,0}, b^{1,-1})^T.$$

Relationship between Cartesian and spherical coordinates is

$$u_1 = r\cos\varphi\sin\vartheta,$$
$$u_2 = r\sin\varphi\sin\vartheta,$$
$$u_3 = r\cos\vartheta.$$

As in the 2D case, we put $r=1$ in further calculations.

3. Calculation of the transition matrix A_p according to (22). As a result of the previous step, we get the transition matrix

$$A_3 = \begin{pmatrix}
-\sqrt{\frac{\pi}{35}} & 0 & \frac{\sqrt{3\pi}}{5} & 0 & \frac{-\sqrt{3\pi}}{5} & 0 & \sqrt{\frac{\pi}{35}} & \frac{-\sqrt{6\pi}}{5} & 0 & \frac{\sqrt{6\pi}}{5} \\
-i\sqrt{\frac{\pi}{35}} & 0 & \frac{-i}{5}\sqrt{\frac{3\pi}{7}} & 0 & \frac{-i}{5}\sqrt{\frac{3\pi}{7}} & 0 & -i\sqrt{\frac{\pi}{35}} & \frac{i}{5}\sqrt{6\pi} & 0 & \frac{i}{5}\sqrt{6\pi} \\
0 & 0 & 0 & \frac{4\sqrt{\frac{\pi}{7}}}{5} & 0 & 0 & 0 & 0 & \frac{2\sqrt{3\pi}}{5} & 0 \\
i\sqrt{\frac{\pi}{35}} & 0 & \frac{-i}{5}\sqrt{\frac{\pi}{21}} & 0 & \frac{-i}{5}\sqrt{\frac{\pi}{21}} & 0 & i\sqrt{\frac{\pi}{35}} & \frac{i}{5}\sqrt{\frac{2\pi}{3}} & 0 & \frac{i}{5}\sqrt{\frac{2\pi}{3}} \\
0 & \sqrt{\frac{2\pi}{105}} & 0 & \frac{-2\sqrt{\frac{\pi}{7}}}{5} & 0 & \sqrt{\frac{2\pi}{105}} & 0 & 0 & \frac{2\sqrt{\frac{\pi}{3}}}{5} & 0 \\
\sqrt{\frac{\pi}{35}} & 0 & \frac{\sqrt{\frac{\pi}{21}}}{5} & 0 & \frac{-\sqrt{\frac{\pi}{21}}}{5} & 0 & -\sqrt{\frac{\pi}{35}} & \frac{-\sqrt{\frac{2\pi}{3}}}{5} & 0 & \frac{\sqrt{\frac{2\pi}{3}}}{5} \\
0 & -\sqrt{\frac{2\pi}{105}} & 0 & \frac{-2\sqrt{\frac{\pi}{7}}}{5} & 0 & -\sqrt{\frac{2\pi}{105}} & 0 & 0 & \frac{2\sqrt{\frac{\pi}{3}}}{5} & 0 \\
0 & 0 & \frac{-4\sqrt{\frac{\pi}{21}}}{5} & 0 & \frac{4\sqrt{\frac{\pi}{21}}}{5} & 0 & 0 & \frac{-\sqrt{\frac{2\pi}{3}}}{5} & 0 & \frac{\sqrt{\frac{2\pi}{3}}}{5} \\
0 & 0 & \frac{4i}{5}\sqrt{\frac{\pi}{21}} & 0 & \frac{4i}{5}\sqrt{\frac{\pi}{21}} & 0 & 0 & \frac{i}{5}\sqrt{\frac{2\pi}{3}} & 0 & \frac{i}{5}\sqrt{\frac{2\pi}{3}} \\
0 & -i\sqrt{\frac{2\pi}{105}} & 0 & 0 & 0 & i\sqrt{\frac{2\pi}{105}} & 0 & 0 & 0 & 0
\end{pmatrix}.$$

4. Calculation of the forms $\mathbf{f}_p$ according to (23) by means of (6) and (7). The elements of new vector of forms $\mathbf{f}_3$ are

$$f_3^{3,3} = \frac{4\pi^{\frac{7}{2}}(i\,m_{030} + 3\,m_{120} - 3\,i\,m_{210} - m_{300})}{3\sqrt{35}\,m_{000}},$$
$$f_3^{3,2} = \frac{4\sqrt{\frac{2}{105}}\pi^{\frac{7}{2}}(-m_{021} + 2\,i\,m_{111} + m_{201})}{m_{000}},$$
$$f_3^{3,1} = \frac{4\pi^{\frac{7}{2}}(-4\,i\,m_{012} + i\,m_{030} - 4\,m_{102} + m_{120} + i\,m_{210} + m_{300})}{5\sqrt{21}\,m_{000}},$$
$$f_3^{3,0} = \frac{8\pi^{\frac{7}{2}}(2\,m_{003} - 3\,(m_{021} + m_{201}))}{15\sqrt{7}\,m_{000}},$$
$$f_3^{3,-1} = \frac{4\pi^{\frac{7}{2}}(-4\,i\,m_{012} + i\,m_{030} + 4\,m_{102} - m_{120} + i\,m_{210} - m_{300})}{5\sqrt{21}\,m_{000}},$$
$$f_3^{3,-2} = \frac{-4\sqrt{\frac{2}{105}}\pi^{\frac{7}{2}}(m_{021} + 2\,i\,m_{111} - m_{201})}{m_{000}},$$
$$f_3^{3,-3} = \frac{4\pi^{\frac{7}{2}}(i\,m_{030} - 3\,m_{120} - 3\,i\,m_{210} + m_{300})}{3\sqrt{35}\,m_{000}},$$
$$f_3^{1,1} = \frac{\frac{-4i}{5}\sqrt{\frac{2}{3}}\pi^{\frac{7}{2}}(m_{012} + m_{030} - i\,(m_{102} + m_{120} + i\,m_{210} + m_{300}))}{m_{000}},$$
$$f_3^{1,0} = \frac{8\pi^{\frac{7}{2}}(m_{003} + m_{021} + m_{201})}{5\sqrt{3}\,m_{000}},$$
$$f_3^{1,-1} = \frac{4\sqrt{\frac{2}{3}}\pi^{\frac{7}{2}}(-i\,m_{012} - i\,m_{030} + m_{102} + m_{120} - i\,m_{210} + m_{300})}{5\,m_{000}}.$$

The forms $f_3^{3,i}$ for $i = 3,2,1,0,-1,-2,-3$ are transformed according to irreducible representation $D^{(3)}$ and the forms $f_3^{1,i}$ for $i = 1,0,-1$ are transformed according to $D^{(1)}$.

5. Explanation and examples. The invariants are again functions which are transformed according to the irreducible representation $D^{(0)}$. According to (17), we can get $D^{(0)}$, for example, in decomposition of tensor product of two irreducible representations $D^{(3)}$:

$$D^{(3\times3)} = D^{(0)} \oplus D^{(1)} \oplus \ldots \oplus D^{(6)}.$$

The form transforming according to the irreducible representation $D^{(0)}$ is then given just by substitution of Clebsch-Gordan coefficients into (15):

$$\begin{aligned}(2f_3^{3,3}f_3^{3,-3} - 2f_3^{3,2}f_3^{3,-2} + 2f_3^{3,1}f_3^{3,-1} - f_3^{3,0^2})/\sqrt{7} = \\ (m_{003}{}^2 + 6\,m_{012}{}^2 + 6\,m_{021}{}^2 + m_{030}{}^2 + 6\,m_{102}{}^2 \\ + 15\,m_{111}{}^2 - 3\,m_{102}\,m_{120} + 6\,m_{120}{}^2 \\ - 3\,m_{021}\,m_{201} + 6\,m_{201}{}^2 - 3\,m_{003}\,(m_{021} + m_{201}) \\ - 3\,m_{030}\,m_{210} + 6\,m_{210}{}^2 \\ - 3\,m_{012}\,(m_{030} + m_{210}) - 3\,m_{102}\,m_{300} \\ - 3\,m_{120}\,m_{300} + m_{300}{}^2)/m_{000}{}^2.\end{aligned} \tag{24}$$

Note that this invariant belongs to the pure rotation invariants presented in [11]. Like in the 2D case, this

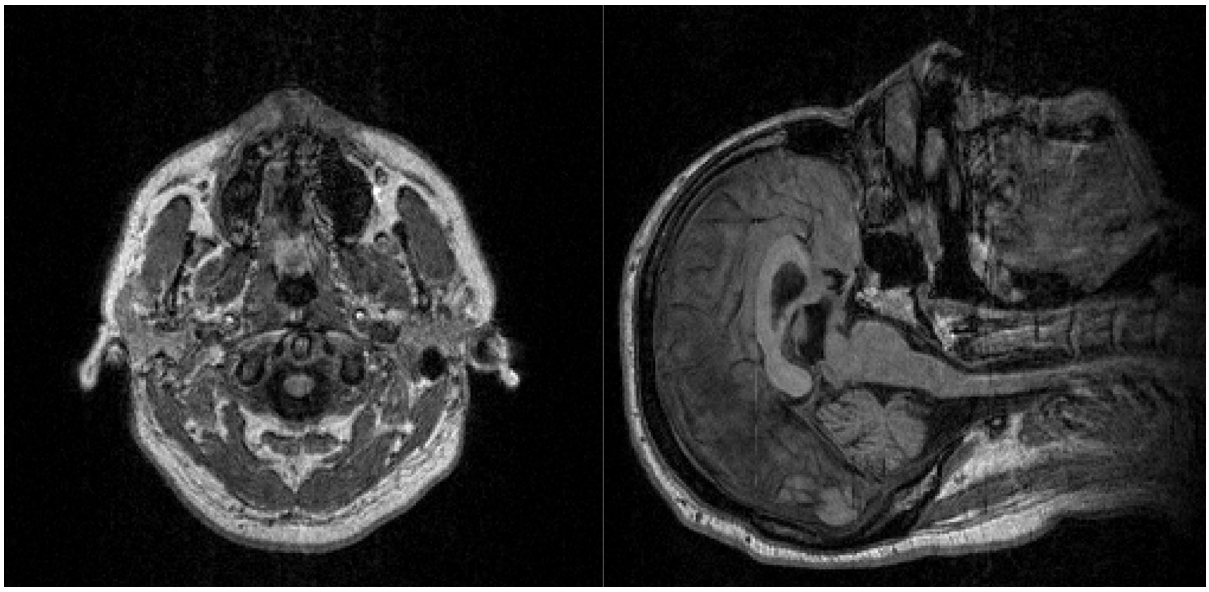

Fig. 1. Original MRI data of a human head: 157th axial slice (left) and 130th sagittal slice (right).

correspondence holds only for third-order invariants. The rotation invariants of higher orders derived by the method [11] and those containing even-order moments are not invariant to convolution.

We present just this one example in explicit form, because most of the other formulae are too complicated. However, the general scheme of deriving invariants remains the same.

6 Experiments

In this section, we study numerical properties of the proposed invariants, namely their invariance to various PSF's and rotations and their robustness to additive noise. Furthermore, we demonstrate that the proposed invariants can be used as a powerful tool for registration of blurred images via template matching.

6.1 Test of Invariance and Discriminability

In this experiment, we demonstrate the invariance to convolution and rotation and the discrimination power of the invariants. As a test data, we used a 3D magnetic resonance image (MRI) of a human head whose size was $256 \times 256 \times 256$ voxels. Two perpendicular slices are depicted in Fig. 1.

This experiment was performed on an object of the size $45 \times 63 \times 38$ voxels that was segmented from the original image. In the following text it is denoted as P. Two slices of P corresponding to the original slices from Fig. 1 are shown in Fig. 2.

In the experiment we used six 3D invariants of the third order constructed by the method that was explained in Section 5.2. Instead of the ordinary moments, we used central moments which also ensure shift invariance. Since their explicit formulae are too complicated, we present them in symbolic form.

Let us denote one particular $D^{(J)}$ on the right-hand side of (17) as

$$\left(D^{(j_1)} \otimes D^{(j_2)}\right)^{(J)}.$$

Then, the combined invariants we used here can be calculated as the basis of the following representations:

$$\begin{aligned}
&(D^{(3)} \otimes D^{(3)})^{(0)},\\
&(D^{(1)} \otimes D^{(1)})^{(0)},\\
&((D^{(3)} \otimes D^{(3)})^{(2)} \otimes (D^{(3)} \otimes D^{(3)})^{(2)})^{(0)},\\
&((D^{(3)} \otimes D^{(1)})^{(2)} \otimes (D^{(3)} \otimes D^{(1)})^{(2)})^{(0)},\\
&((D^{(3)} \otimes D^{(3)})^{(2)} \otimes (D^{(3)} \otimes D^{(1)})^{(2)})^{(0)},\\
&((D^{(3)} \otimes D^{(1)})^{(2)} \otimes (D^{(1)} \otimes D^{(1)})^{(2)})^{(0)}.
\end{aligned}$$

The image P was rotated in all Euler angles by the same angle α (where $\alpha = 0, 5, 10, 15, \cdots, 90$, respectively) and blurred by Gaussian mask of parameter σ (where $\sigma = 0, 1, 2, \cdots, 7$, respectively). Then, the distance in the space of invariants between each both transformed and blurred version and the original image was calculated. The sum of relative deviations d_r of the invariants was used as a distance measure. Since the influence of rotation is much stronger than the influence of blurring, we visualized the results separately in two graphs (see Figs. 3 and 4). As can be seen from the graphs, the relative deviations of the invariants are very small in all cases, which is in accordance with the theoretical expectation. Higher errors for some values of the rotation angle are caused by resampling when rotating the image.

Fig. 2. The test object P: Axial (left) and sagittal (right) slices.

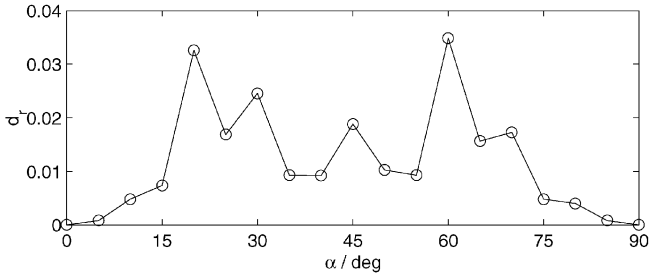

Fig. 3. Relative distance d_r between P and its rotated versions ($\sigma = 0$).

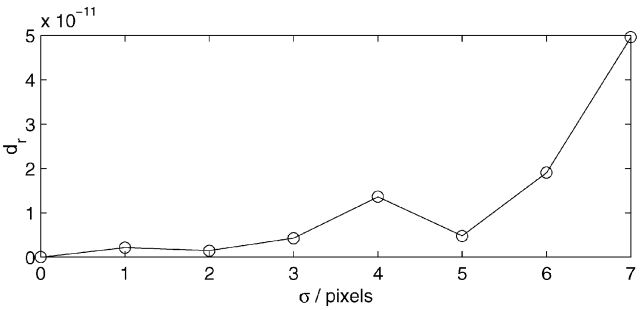

Fig. 4. Relative distance d_r between P and its blurred versions ($\alpha = 0$).

Finally, we show that the relative errors occurring due to image rotation and filtering are substantially smaller than the "distance" between two different images, which means that the discrimination power of the invariants is not degraded by the above mentioned image transformations. The values of relative deviations of the individual invariants for some illustrative examples are presented in Table 1. The deviations are calculated as in the previous case between the original P and P convolved with various masks. The last two columns show the deviations between P and two randomly chosen parts of the original image of the same size as P. From the last row of the table, it is obvious that the proposed invariants are sufficiently discriminative.

6.2 Test of Robustness

The next experiment investigates the robustness of the proposed invariants to additive noise (Gaussian white noise was used in this experiment). To describe the impact of noise on the image, we used signal to noise ratio

$$\mathrm{SNR[dB]} = 10 \log_{10} \frac{\text{variance of the image}}{\text{variance of the noise}}.$$

We corrupted the image P gradually by noise with various SNR. For each particular value of SNR, 50 realizations of noise were generated and the values of the invariants were calculated. The statistical behavior (mean and standard deviation) of the relative distance between the original and noisy images is depicted in Fig. 5.

Two important observations can be done from Fig. 5. First, the error caused by noise was in all tested cases significantly higher than that induced by convolution and/or rotation. This is obvious because the invariants cannot be "strictly invariant" to noise. Second, the error is still much lower than the "distance" of two different images (note that usually in practice the meaningful levels of SNR are higher than 10 dB).

6.3 Template Matching

In this experiment, the template matching test was performed. A randomly chosen spherical part of the original MRI image of the diameter 31 pixels was used as a template. The original image was rotated by 30 degrees in all Euler angles, blurred by Gaussian masks of various sizes and corrupted by additive noise. The template was shifted across the image and in each its position the invariants of the corresponding part of the image were calculated and compared with the invariants of the template. Thanks to the rotation invariance of the features, template rotation need not be performed. The "matching position" was localized as that with minimum d_r.

The matching accuracy depends on the SNR (which is obvious) and on the size of the blurring mask. This is because the voxels near the template boundary are affected by the voxels from the outside. This boundary effect of course increases when the blurring becomes larger. The localization errors for various blurring sizes and SNRs are depicted in Fig. 6. One may observe that if the size of the blurring mask is not too large with respect to the size of the template, the results are very good, even if noise is present.

We conducted a similar experiment in which we studied the influence of rotation angle and the shape of the blurring masks on the localization error (note that, from a theoretical point of view, our invariants are invariant to all blurring functions having the central symmetry, including anisotropic blurring). The MRI image was rotated in all Euler angles by the angle α (where $\alpha = 0, 5, 10, 15, \cdots, 90$, respectively) and blurred by various anisotropic masks. It can be seen from Fig. 7 that even if the rotation is big and the major blurring direction changes, the localization error is still kept reasonably low.

TABLE 1

	(a)	(b)	(c)	(d)	(e)	(f)
1	6.47 e-16	2.72 e-15	1.03 e-15	2.20 e-15	0.834	0.721
2	4.34 e-14	2.54 e-14	3.87 e-14	4.26 e-14	0.610	0.558
3	3.19 e-14	3.82 e-14	3.17 e-14	3.76 e-14	0.920	0.672
4	4.23 e-14	2.38 e-14	4.23 e-14	3.92 e-14	0.702	0.808
5	2.09 e-14	7.96 e-15	1.78 e-14	1.89 e-14	0.952	0.765
6	9.76 e-14	9.66 e-14	1.42 e-13	1.01 e-13	0.867	0.487
d_r	2.37 e-13	1.95 e-13	2.73 e-13	2.42 e-13	4.89	4.01

Relative deviations of the individual invariants whose indices are in the left column. In the bottom row is the total relative distance from P. Convolution masks: (a) $5 \times 5 \times 5$ averaging, (b) $5 \times 5 \times 5$ of ones with 3D cross of zeros in the middle, (c) $5 \times 5 \times 5$ of ones with both upper and bottom boundary negative, (d) $5 \times 5 \times 5$ Gaussian with parameter σ = 1 pixel, (e) and (f) randomly chosen parts of the original image of the same size as P.

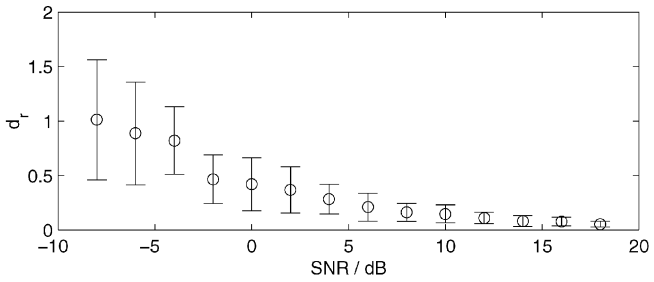

Fig. 5. Relative distance d_r between original image P and its noisy versions.

Finally, we extended the matching experiment to more templates. Eight spherical templates of 15-pixel radius were manually extracted from the original MRI data. The original image was then rotated around all three axes by 30 degrees and blurred by anisotropic Gaussian mask with standard deviations [0.5 0.5 0.2]. We looked for the matching position of each template by an exhaustive search within the whole image—no estimation of approximate matching position was used. The results were really encouraging: the positions of five templates were found accurately and in the three other cases the error was one pixel.

The experiments described in this Section proved that the proposed invariants can be used successfully in 3D template matching regardless of rotation and/or blurring of the images involved. There are however, some limitations posed mainly by boundary effect and, of course, by noise if it is heavy. In all of these experiments we were using six invariants only. The results can be further improved by employing more invariants, but the higher the order the less robustness of the respective moments.

6.4 Image Registration

In the last experiment, a successful utilization of the combined invariants in registration of out-of-focused 2D images is demonstrated.

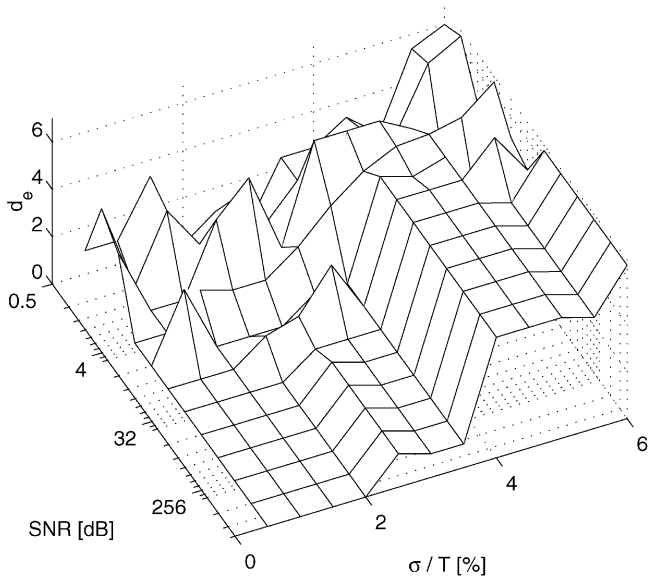

Fig. 6. Template matching test: d_e—localization error (Euclidean distance from the correct position), σ—standard deviation of the Gaussian blurring mask, σ/T—the ratio of the blur and the template size (in %).

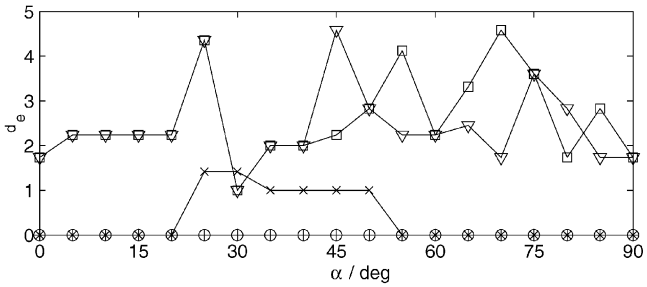

Fig. 7. Template matching with anisotropic blurring: d_e—localization error (Euclidean distance from the correct position), α—rotation angle, ◯—no blurring, $\times$—blurring by $1 \times 1 \times 3$ mask after rotation, $+$—blurring by $1 \times 1 \times 3$ mask before rotation, □—blurring by $3 \times 3 \times 5$ mask after rotation, ▽—blurring by $3 \times 3 \times 5$ mask before rotation.

The problem to be solved is to estimate the motion parameters and the current position of the camera in the real indoor scene. The camera, which takes one frame every second, moves parallel to the wall and rotates. The system monitors the scene and looks for alien objects which may appear in the view of the camera. When such an object appears in front of the camera, the camera is automatically focused on it. Thus, the rest of the scene becomes out-of-focused (see Fig. 8). Position estimation can be resolved via registration of the initial (reference) frame and the image acquired at the moment when the object has appeared. The registration parameters (mutual rotation and shift of the reference and current frames) then unambiguously determine the actual camera position.

The registration proceeds as follows: First, control point candidates (CPC's) are detected both in the initial and the current frames. Significant corners and other corner-like dominant points are considered as the candidates. To detect them, a method developed particularly for blurred images [36] is employed. In this experiment we detected 30 CPC's in each frame.

Second, the correspondence between the CPC's sets must be established and the candidates having no counterparts should be rejected. To do that, a vector of invariants is computed for each CPC over its circular neighborhood (here, three third-order invariants and two fifth-order ones were employed) and then the CPC's are matched in the space of the invariants by minimum-distance rule or by any more sophisticated technique (in this experiment we applied robust matching by means of so-called likelihood coefficients [37]). Once the control point (CP) correspondence is established, their positions can be refined by a local search in their neighborhoods. For every pixel from the neighborhood, its invariant vector is calculated. The point having the minimum distance to the invariant vector of the CP counterpart is set as the refined position of the CP. If the subpixel accuracy is required, it can be achieved by an appropriate interpolation in the distance matrix.

Finally, as soon as the control point correspondence is established and their coordinates refined, we can find an "optimal" rotational-translational mapping whose parameters are calculated via least-square fit. Knowing these parameters and the initial camera position, the current position can be easily estimated.

We repeated this experiment six times changing the camera rotation and the distance of the inserted object (i.e., the amount of blurring of the background). The results were

Fig. 8. Images of the indoor scene. Camera at the initial position (left); camera at an unknown position, the scene is out-of-focused due to the inserted object (right). 30 CPC's are marked by crosses, those which form the corresponding CP pairs are numbered.

evaluated by the comparison with ground truth. In all cases the estimates correspond well to the reference values. The errors are mostly below the discretization error. For illustration, in the situation depicted in Fig. 8, the ground-truth registration parameters were rotation $10.92°$, vertical translation 37.7 pixels, and horizontal translation 41.2 pixels, while the computed parameters were $11.00°$, 37.7 pixels, and 41.0 pixels, respectively. Summarizing the results of all six experiments, the mean error and standard deviation of the estimation of rotation angle were $0.06°$ and $0.05°$, the same for vertical translation were 0.1 and 0.4 pixel, and for horizontal translation 0.3 and 0.5 pixel.

In a comparative experiment, we used exactly the same registration algorithm, but invariants only to rotation [3] were used instead of our combined invariants. None of the six studied cases was correctly resolved. In all cases, many CP pairs were matched incorrectly. For instance, in the experiment in Fig. 8, CP no. 7 was mismatched to the unlabeled CPC to the left from no. 8. This illustrates the actual need of blur invariants when attempting to register blurred images.

It is worth noting a few empiric observations. The above described registration algorithm has several user-defined parameters: the choice and the number of the invariants involved, the radius of the neighborhood the invariants are calculated from, and the radius of the neighborhood used for the CP's positions refinement. The choice of the parameters is influenced by the type of the scene and an extent of the camera motion and the blurring degradation, among others. However, there is no explicit relationship between parameter values and the type of image deformation, just heuristic conclusions can be made. The experiments we have performed indicate that from three to nine invariants usually provide sufficient discriminative power. The more blurred the image is, the larger neighborhood for calculating the invariants should be (common values range from 30 to 90 pixels). There is no "optimal" radius, generally the larger neighborhood provides better discrimination power. For a particular image, upper limit is set up by the homogeneity constraint (the amount of blurring can be different for different neighborhoods but should not vary within each of them) and by the required complexity. The neighborhoods for position improvement should be small (2 or 3 pixel radius) because the corner detection algorithm should not produce higher deviations of the candidate positions.

It should also be noted that, in this experiment, the degrees of freedom of the camera motion were limited to along-axis rotation and movement parallel to the wall of the room. Thus, rotation and blurring invariance of the proposed descriptors was sufficient. In case of unrestricted camera motion in 3D space, projective (or at least affine) invariant descriptors along with a method for invariant neighborhood selection would be desirable. This is, however, a difficult problem which has been partially resolved recently for isolated planar objects in [38], but the general case is still under investigation.

7 Conclusion

The paper is devoted to the image features which are invariant simultaneously to convolution with a centrally symmetric filter and rotation. There is no demand of a prior knowledge of the size, shape, and coefficients of the convolution filter (with exception of the centrosymmetry). There is also no limitation of the dimensionality—the invariants can be derived for images of arbitrary dimension. First, we presented recursively defined moment-based features invariant to convolution. Then, we employed group representation theory to derive forms of the blur invariants, which are then invariant also to rotation. In the experimental part, we concentrated our attention to 3D case. We demonstrated the invariance properties in case of various convolution filters, the robustness to additive noise, and the discrimination power. We showed a successful utilization of the invariants when registering blurred and noisy MRI data and demonstrated how the invariants can be used for registration of out-of-focused 2D images of an indoor scene.

The benefit of the paper is twofold. From a theoretical point of view, this paper as the first one bridges the gap between pure convolution invariants presented by Flusser et al. [25], [33] and pure rotation invariants proposed in [11], [19]. From a practical point of view, the invariants presented in this paper are more applicable thanks to their invariance to broader class of image degradations. We envisage the applications mainly in registration of images taken by nonideal sensors and in

object recognition in blurred and noisy environment. There are many application areas where one has to deal with blurred images: satellite images are often blurred due to the composite sensor PSF and atmospheric turbulence [39] and astronomical images are also degraded by a low-pass filtering due to nonideal observational conditions [40]. As it was shown in Section 6, the proposed method can be applied to registration of volumetric medical images as well as of 2D images degraded by blurring of an unknown nature. On the other hand, it was demonstrated that traditional rotation moment invariants cannot resolve this task successfully. To speed up the process when registering large images, popular multiscale techniques [41] along with effective search strategies [42], [43] can be employed. Another possible application is character/digit recognition on blurred images and in the area of video surveillance and person authentication where face recognition from defocused photographs is often required.

However, our method has certain limitations. In image registration, the invariants are calculated from parts of the image only (usually from the neighborhoods of certain significant points). In such a case, the gray values along the boundaries of these parts are influenced by the pixels from the outside and convolution is not well defined within the region of interest. The robustness to this so-called "boundary effect" depends on the size of the region of interest and on the size of the blurring filter. The robustness may be low when both sizes are comparable, which prevents from using the blur invariants in such cases. In face and character recognition tasks, the limitation is induced by the fact that our invariants (as well as all other moment-based invariants) are intrinsically global, i.e., they are calculated from the whole image including background. Thus, the object must be segmented from the background prior the calculation of the invariants (which may be problematical in case of heavy blur) or, alternatively, the background must be the same for all objects entering the system.

Another limitation appears when we want to distinguish among symmetric objects. It has a profound theoretical reason—any shape descriptor invariant to a certain class of transformations cannot, in principle, distinguish objects which differ from each other only by transformations from this class. Thus, any invariant (even different from those presented here) to convolution with a centrosymmetric PSF cannot distinguish different centrosymmetric objects because it must give a constant response on all centrosymmetric images. This is because any centrosymmetric image can be considered as a blurring PSF acting on delta-function.

The forms of the invariants presented in this paper are not invariant to image scaling. Scaling invariance can be achieved easily just by proper normalization of the moments, but another more serious problem appears when we want to register/match images having a scale difference. The neighborhoods of the control points must also be scale-invariant which is difficult to ensure.

The assumption of centrosymmetry of the degradation filter is not a significant limitation for practical utilization of the method. Most real sensors and imaging systems, both optical and nonoptical ones, have the PSF with certain degree of symmetry. In many cases they have even higher symmetries, such as axial or radial symmetry. Thus, the central symmetry is general enough to describe almost all practical situations. It should be pointed out that although our primary motivation was to find invariants to low-pass blurring, the invariants described in this paper are applicable to any centrosymmetric PSF having nonzero integral, even if it has negative values.

ACKNOWLEDGMENTS

This work has been supported by the Grant Agency of the Czech Republic under the projects No. 102/00/1711 and No. 102/01/PO65.

The authors would like to thank to T. Novotný and K. Netočný for critical reading of the manuscript and helpful comments, to J. Kautsky for many inspiring discussions, to I. Hollander for kindly providing the MRI data, to S. Saic for his help with the indoor images acquisition, and to four anonymous reviewers for their constructive criticism.

REFERENCES

[1] J.L. Mundy and A. Zisserman, *Geometric Invariance in Computer Vision*. MIT Press, 1992.
[2] T.H. Reiss, *Recognizing Planar Objects using Invariant Image Features.* Berlin: Springer, 1993.
[3] M.K. Hu, "Visual Pattern Recognition by Moment Invariants," *IRE Trans. Information Theory*, vol. 8, pp. 179-187, 1962.
[4] Y.S. Abu-Mostafa and D. Psaltis, "Recognitive Aspects of Moment Invariants," *IEEE Trans. Pattern Analysis and Machine Intelligence,* vol. 6, pp. 698-706, 1984.
[5] M.R. Teague, "Image Analysis via the General Theory of Moments," *J. Optical Soc. Am.*, vol. 70, pp. 920-930, 1980.
[6] C.H. Teh and R.T. Chin, "On Image Analysis by the Method of Moments," *IEEE Trans. Pattern Analysis and Machine Intelligence,* vol. 10, pp. 496-513, 1988.
[7] S.O. Belkasim, M. Shridhar, and M. Ahmadi, "Pattern Recognition with Moment Invariants: A Comparative Study and New Results," *Pattern Recognition,* vol. 24, pp. 1117-1138, 1991.
[8] A. Khotanzad and Y.H. Hong, "Invariant Image Recognition by Zernike Moments," *IEEE Trans. Pattern Analysis and Machine Intelligence,* vol. 12, pp. 489-497, 1990.
[9] J. Flusser and T. Suk, "Pattern Recognition by Affine Moment Invariants," *Pattern Recognition,* vol. 26, pp. 167-174, 1993.
[10] F.A. Sadjadi and E.L. Hall, "Three Dimensional Moment Invariants," *IEEE Trans. Pattern Analysis and Machine Intelligence,* vol. 2, pp. 127-136, 1980.
[11] C.H. Lo and H.S. Don, "3-D Moment Forms: Their Construction and Application to Object Identification and Positioning," *IEEE Trans. Pattern Analysis and Machine Intelligence,* vol. 11, pp. 1053-1064, 1989.
[12] X. Guo, "3-D Moment Invariants Under Rigid Transformation," *Proc. Fifth Int'l Conf. Computer Analysis of Images and Patterns '93,* pp. 518-522, 1993.
[13] J.M. Galvez and M. Canton, "Normalization and Shape Recognition of Three Dimensional Objects by 3-D Moments," *Pattern Recognition,* vol. 26, pp. 667-681, 1993.
[14] T.H. Reiss, "Features Invariant to Linear Transformations in 2D and 3D," *Proc. 11th Int'l Conf. Pattern Recognition '92,* vol. III, pp. 493-496, 1992.
[15] G. Taubin and D.B. Cooper, "Object Recognition Based on Moment (or Algebraic) Invariants," *Geometric Invariance in Computer Vision,* J.L. Mundy and A.Zisserman, eds., MIT Press, pp. 375-397, 1992.
[16] V. Markandey and R.J.P. deFigueiredo, "Robot Sensing Techniques Based on High-Dimensional Moment Invariants and Tensors," *IEEE Trans. Robotics and Automation,* vol. 8, pp. 186-195, 1992.
[17] A.G. Mamistvalov, "On the Fundamental Theorem of Moment Invariants," *Bull. Academic Science Georgian SSR,* vol. 59, pp. 297-300, 1970.
[18] T.H. Reiss, "The Revised Fundamental Theorem of Moment Invariants," *IEEE Trans. Pattern Analysis and Machine Intelligence,* vol. 13, pp. 830-834, 1991.
[19] A.G. Mamistvalov, "n-Dimensional Moment Invariants and Conceptual Mathematical Theory of Recognition n-Dimensional Solids," *IEEE Trans. Pattern Analysis and Machine Intelligence,* vol. 20, pp. 819-831, 1998.

[20] A.G. Mamistvalov, "On the Construction of Affine Invariants of *n*-Dimensional Patterns," *Bull. Academic Science Georgian SSR,* vol. 76, pp. 61-64, 1974.
[21] L. van Gool, T. Moons, and D. Ungureanu, "Affine/Photometric Invariants for Planar Intensity Patterns," *Proc. Fourth European Conf. Computer Vision,* pp. 642-651, Springer, 1996.
[22] F. Mindru, T. Moons, and L. van Gool, "Recognizing Color Patterns Irrespective of Viewpoint and Illumination," *Proc. IEEE Conf. Computer Vision and Pattern Recognition,* vol. 1, pp. 368-373, 1999.
[23] S. Paschalakis and P. Lee, "Combined Geometric Transformation and Illumination Invariant Object Recognition," *Proc. 15th Int'l Conf. Pattern Recognition,* pp. 588-591, 2000.
[24] E. Bigorgne, C. Achard, and J. Devars, "An Invariant Local Vector for Content-Based Image Retrieval," *Proc. 15th Int'l Conf. Pattern Recognition,* pp. 1019-1022, 2000.
[25] J. Flusser and T. Suk, "Degraded Image Analysis: An Invariant Approach," *IEEE Trans. Pattern Analysis and Machine Intelligence,* vol. 20, pp. 590-603, 1998.
[26] J. Flusser, T. Suk, and S. Saic, "Recognition of Blurred Images by the Method of Moments," *IEEE Trans. Image Processing,* vol. 5, pp. 533-538, 1996.
[27] Y. Zhang, C. Wen, and Y. Zhang, "Estimation of Motion Parameters from Blurred Images," *Pattern Recognition Letters,* vol. 21, pp. 425-433, 2000.
[28] Y. Zhang, C. Wen, Y. Zhang, and Y.C. Soh, "Determination of Blur and Affine Combined Invariants by Normalization," *Pattern Recognition,* vol. 35, pp. 211-221, 2002.
[29] J. Lu and Y. Yoshida, "Blurred Image Recognition Based on Phase Invariants," *IEICE Trans. Fundamentals of El. Comm. and Comp. Sci.,* vol. E82A, pp. 1450-1455, 1999.
[30] Y. Zhang, Y. Zhang, and C. Wen, "A New Focus Measure Method Using Moments," *Image and Vision Computing,* vol. 18, pp. 959-965, 2000.
[31] J. Flusser and B. Zitová, "Combined Invariants to Linear Filtering and Rotation," *Int'l J. Pattern Recognition Artificial Intelligence,* vol. 13, pp. 1123-1136, 1999.
[32] J. Flusser, B. Zitová, and T. Suk, "Invariant-Based Registration of Rotated and Blurred Images," *Proc. IEEE Int'l Geoscience and Remote Sensing Symp.,* I.S. Tammy, ed., pp. 1262-1264, 1999.
[33] J. Flusser, J. Boldyš, and B. Zitová, "Invariants to Convolution in Arbitrary Dimensions," *J. Math. Imaging and Vision,* vol. 13, pp. 101-113, 2000.
[34] J.P. Elliot and P.G. Dawber, *Symmetry in Physics.* London: MacMillan, 1979.
[35] J. Flusser, "On the Independence of Rotation Moment Invariants," *Pattern Recognition,* vol. 33, pp. 1405-1410, 2000.
[36] B. Zitová, J. Kautsky, G. Peters, and J. Flusser, "Robust Detection of Significant Points in Multiframe Images," *Pattern Recognition Letters,* vol. 20, no. 2, pp. 199-206, 1999.
[37] J. Flusser, "Object Matching by Means of Matching Likelihood Coefficients," *Pattern Recognition Letters,* vol. 16, pp. 893-900, 1995.
[38] T. Suk and J. Flusser, "Features Invariant Simultaneously to Convolution and Affine Transformation," *Proc. Ninth Int'l Conf. Computer Analysis of Images and Patterns '01,* W. Skarbek, ed., pp. 183-190, Springer, 2001.
[39] S.E. Reichenbach, D.E. Koehler, and D.W. Strelow, "Restoration and Reconstruction of AVHRR Images," *IEEE Trans. Geoscience and Remote Sensing,* vol. 33, pp. 997-1007, 1995.
[40] R. Krejčí, S. Šimberová, and J. Flusser, "A New Multichannel Blind Deconvolution Method and its Application to Solar Images," *Proc. 14th Int'l Conf. Pattern Recognition,* A. Jain, S. Venkatesh, and B.C. Lovell, eds., pp. 1765-1767, 1998.
[41] R.Y. Wong and E.L. Hall, "Sequential Hierarchical Scene Matching," *IEEE Trans. Computers,* vol. 27, pp. 359-366, 1978.
[42] H.S. Sawhney and R. Kumar, "True Multi-Image Alignment and Its Applications to Mosaicing and Lens Distortion Correction," *IEEE Trans. Pattern Analysis and Machine Intellingence,* vol. 21, pp. 235-243, 1999.
[43] W.H. Press, S.A. Teukolsky, W.T. Vetterling, and B.P. Flannery, *Numerical Recipes in C: The Art of Scientific Computing.* Cambridge Univ. Press, 1993.

Jan Flusser received the MSc degree in mathematical engineering from the Czech Technical University, Prague, Czech Republic in 1985, and the PhD degree in computer science from the Czechoslovak Academy of Sciences in 1990. Since 1985, he has been with the Institute of Information Theory and Automation, Academy of Sciences of the Czech Republic, Prague. Since 1995, he has been holding the position of a head of Department of Image Processing. Since 1991, he has also been affiliated with the Faculty of Mathematics and Physics, Charles University, Prague, where he gives the courses on digital image processing. His current research interests include digital image processing, pattern recognition, and remote sensing. He has authored and coauthored more than 60 research publications in these areas. He is a member of the IEEE, IEEE Computer Society, Signal Processing Society, and Geoscience and Remote Sensing Society.

Jiří Boldyš received the MSc degree in physics from the Charles University, Prague, Czech Republic in 1996, and is currently a PhD candidate in computer physics at the Charles University, Prague, Czech Republic. In 1998, he joined the Institute of Information Theory and Automation, Academy of Sciences of the Czech Republic. Since 2000, he has been with the Laboratory of Media Technology, Helsinki University of Technology, Finland. His current research interests include theory of invariants, wavelets, surveillance applications, and image understanding.

Barbara Zitová received the MSc degree in computer science from the Charles University, Prague, Czech Republic in 1995 and the PhD degree in software systems from the Charles University, Prague, Czech Republic in 2000. Since 1995, she has been with the Institute of Information Theory and Automation, Academy of Sciences of the Czech Republic, Prague. She also gives tutorials on image processing and pattern recognition at the Czech Technical University and participates in the courses on Digital Image Processing at the Faculty of Mathematics and Physics, Charles University. Her current research interests include image processing, geometric invariants, image enhancement, and image registration. She has authored/coauthored more than 20 research publications in these areas. She is a member of the IEEE.